Boat acceleration, temporal structure of the stroke cycle, and effectiveness in rowing

V Kleshnev
BioRow Ltd, 4 Egerton Road, Slough, Berkshire SL2 2LD, UK. email: kleval@btinternet.com

The manuscript was received on 25 January 2009 and was accepted after revision for publication on 23 September 2009.

DOI: 10.1243/17543371JSET40

Abstract: The purposes of the study were to explain the double peak in the boat acceleration during the drive phase, to analyse the temporal structure of the stroke cycle, and to find correlations between the temporal structure and the boat type, rower gender, stroke rate, force profile, and effectiveness of rowing. Measurements of the boat acceleration, boat velocity, handle force, oar angle, and velocity of body segments were made in competitive rowing boats using a telemetry system. The accelerations of the whole system and of the rower's centre of mass (CM) were derived and used to define the temporal structure of the stroke cycle. Six microphases were defined during the drive phase, and three microphases were defined during the recovery phase. The relative magnitudes of the accelerations of the boat and of the rower's CM switched twice during the drive phase. During the 'initial rower's acceleration' and the 'rower's acceleration' microphases, the acceleration of the rower's CM was higher and, during the 'initial boat acceleration' and 'boat acceleration' microphases, the acceleration of the boat was higher. The presence of the initial boat acceleration microphase is an important indicator of the effectiveness of a rower's technique.

Keywords: boat acceleration, temporal structure of the stroke cycle, effectiveness in rowing

1 INTRODUCTION

In a temporal or phase analysis, a movement is divided into a sequence of phases and microphases. Each phase has a clearly defined biomechanical function and clearly identified phase boundaries (often called 'key moments' or 'key events') [**1**]. A temporal analysis is a very versatile method of biomechanical analysis and can be applied to many sports. Temporal analysis can play an integrating role for other biomechanical techniques, e.g. by linking kinetic and kinematic measurements obtained using various instruments, such as force platforms with video analysis. Temporal analysis can also reduce the complexity of an analysis of a sporting technique and can aid a coach's or athlete's understanding of a technique.

Temporal analysis is a well-developed technique in a number of cyclic locomotion sports such as running, cycling, swimming, skating, and skiing. The most common definition has two main phases in the cycle: first, the 'propulsive' phase (the 'drive' or 'stroke' phase), where the athlete actively interacts with the support substance (ground, water, snow, or ice) and executes an effort to propel the centre of mass (CM) of the athlete–equipment system forwards; second, the 'non-propulsive' phase (the 'glide' or 'recovery' phase), where resistance forces act alone to decrease the speed of the system CM [**2**]. These two phases may be further divided into microphases. For example, in running, the propulsive phase has been divided into 'foot strike', 'midsupport', and 'take-off' microphases, and the recovery phase has been divided into 'follow-through', 'forward swing', and 'foot descent' microphases [**3**].

Temporal analysis of rowing is not as well developed as it is in other cyclic sports. Muscular activity and body segment sequencing has been used to define microphases ('legs push', 'trunk drive', and 'arm pull') during the drive phase [**4**, **5**]. However, this approach does not link the main propulsion task with the analysis of the timing of the phases.

In the present study, the acceleration of the boat was used to link the main propulsive task with the temporal analysis. Typical patterns of boat acceleration have one period of negative acceleration (i.e. reducing boat velocity) at the catch, and two periods of positive acceleration during the drive and recovery [**6**]. The negative acceleration at the catch and

the positive acceleration during the recovery are explained by the transfer of momentum between the rower's mass and the boat mass (which can move significantly relative to each other). Positive acceleration during the drive phase is explained by the propulsion forces produced by the oars. Boat acceleration during the drive phase is usually not constant; it typically has a first peak, then a short gap, and finally a longer positive peak. Coaches have expressed their concerns about this variation in boat acceleration during the drive, but the reason for this phenomenon is not clear.

The purposes of this study were, first, to explain the double peak in the boat acceleration during the drive phase in rowing, second, to analyse the temporal structure of the stroke cycle in terms of the accelerations of the boat and of the rower's CM, and, third, to find correlations between the temporal structure of the stroke cycle and the boat type, rower gender, stroke rate, force profile, and effectiveness of rowing.

2 METHOD

2.1 Test subjects

The measurements were conducted during 1999–2004 as a part of regular biomechanical assessments of athletes at the Australian Institute of Sport and from the Australian National Rowing Team. The study was approved by the ethics commission, and the athletes were informed about the nature and outcomes of the measurements. A total of 294 crews, both male and female, were measured. Table 1 gives a breakdown of the rowers into the normal rowing groups and key average parameters of those groups. These data were used for the statistical analysis of the temporal structure.

In addition, a series of more detailed assessments were used in this study, with measurements of the stretcher and gate forces in addition to the standard set of measurements. Seven male single scullers with a mean height of 1.89 ± 0.04 m and body mass of 86.4 ± 3.1 kg took part, in addition to their regular biomechanical assessment. These data were used for the definition and explanation of the temporal structure.

2.2 Data acquisition

A radio telemetry system was used for data acquisition. The system consisted of transducers, an electronic unit with signal conditioners and analogue-to-digital converters (12 bit, 25 Hz sampling frequency), and a pair of radio modems. Acquired data were transmitted to a motorboat and stored in real time on the hard disk of a laptop computer. The measurements were made during on-water rowing in standard racing boats [**7**]. The total mass of each boat with riggers, oars, and telemetry system, but without the moveable seat, was estimated for each session. All crews performed an incremental test consisting of four to eight efforts over 250–500 m at a pace of 16–46 strokes/min.

Several relevant mechanical parameters were measured. The boat velocity $\boldsymbol{V}_{\text{boat}}$ was measured using an electromagnetic impeller (Nielsen–Kellerman, Boothwyn, Pennsylvania, USA) which was linked to the telemetry system. The impeller was calibrated during each session by timing the boat over a known distance. The linear calibration regression was calculated using at least two different average boat speeds (accuracy, ±1.0 per cent).

The boat acceleration $\boldsymbol{A}_{\text{boat}}$ was measured along the horizontal axis using an accelerometer (Analog Devices, Norwood, Massachusetts, USA; accuracy, ±1 per cent). The accelerometer was calibrated using three-point linear regression, where the horizontal orientation of the accelerometer was taken as zero and the vertical orientations of the accelerometer in opposite directions were taken as $\pm \boldsymbol{g} = 9.796\ \text{m/s}^2$ [**8**]. The accelerometer was built into the electronics unit, mounted on the boat deck, and aligned along the boat's longitudinal axis. Positive acceleration was taken to be towards the bow of the boat (i.e. when the boat increases its velocity).

The horizontal oar angle A_{h} and vertical oar angle A_{v} were measured using conductive-plastic potentiometers (linearity, ±0.1 per cent) connected to the oar shaft with a light arm and a bracket. The

Table 1 Subjects of the study (the values ± the standard deviations are given for the heights and the body masses)

Gender	Weight	Boat type	n	Height (m)	Body mass (kg)
Male	Heavyweight	Sweep	46	1.943 ± 0.031	91.5 ± 2.4
Male	Heavyweight	Scull	45	1.915 ± 0.045	90.7 ± 4.1
Male	Lightweight	Sweep	36	1.830 ± 0.021	73.0 ± 1.0
Male	Lightweight	Scull	29	1.833 ± 0.028	73.4 ± 1.3
Female	Heavyweight	Sweep	52	1.804 ± 0.028	74.1 ± 2.6
Female	Heavyweight	Scull	44	1.794 ± 0.040	74.2 ± 3.5
Female	Lightweight	Scull	42	1.702 ± 0.032	59.1 ± 1.0

oar angles were calibrated at four or more points using a protractor.

The normal component of the force $\boldsymbol{F}_h$ applied to the handle of the oar was measured using a custom-made strain-gauge-based transducer attached to the oar shaft (accuracy, ±0.5 per cent). Each instrumented oar was dynamically calibrated before each session using a precision load cell to apply a load to the handle. The oar was supported 0.02 m from the collar (at the point corresponding to the centre of contact with the gate), the blade was fixed, and the force applied perpendicular to the oar shaft at the middle of the handle (0.15 m in from the end for a sweep oar; 0.06 m for a sculling oar).

The seat position L_s was measured using a custom-made device, which consisted of a spring-loaded ten-turn potentiometer connected to the seat with a low-stretch line (accuracy, ±0.1 per cent). The position L_t of the top of the trunk was measured in small boats using a device similar to the seat position sensor. The device was attached to the boat deck and the line was passed up through a pulley mounted on a mast and attached to the trunk of the athlete, level with the sternum and clavicle (C7) joint.

2.3 Data processing

The data collected during one test effort were converted into a form representing one typical stroke cycle for the sample [**9**]. In this 'normalization' process the average cycle time was calculated over all the strokes in the sample and then each cycle of the sample was extended or compressed to have the same average cycle time. The cycle start time was defined as the moment when the oar (right oar in sculling) of the stroke rower crosses the zero angle (perpendicular to the boat) during the recovery phase. This moment was used as the start of the stroke cycle for the whole crew. The data were then processed (averaged) into 50-point data arrays for each measured variable (oar angle, force, etc.).

Discrete data values (extremes or microphases) were then derived using second-order polynomial interpolation based on the four nearest points of the arrays. The normalization algorithm was checked for validity by means of a comparison between the derived values (such as catch and release angles, maximum force, work and power) calculated using normalized data and an average of those values from each cycle in the sample using raw data. The differences ranged from 0.02 per cent to 0.85 per cent, which was considered satisfactory.

2.4 Data analysis

A new method was developed to define the acceleration of the rower's CM. The total blade force $\boldsymbol{F}_{bl}$ of the crew was derived from the sum of the measured handle forces $\boldsymbol{F}_h$ multiplied by the ratio of the actual inboard length $L_{in\text{-}a}$ to the outboard length $L_{out\text{-}a}$ (Fig. 1).

Neglecting oar inertia (which is very small during the drive), the total blade force is given by

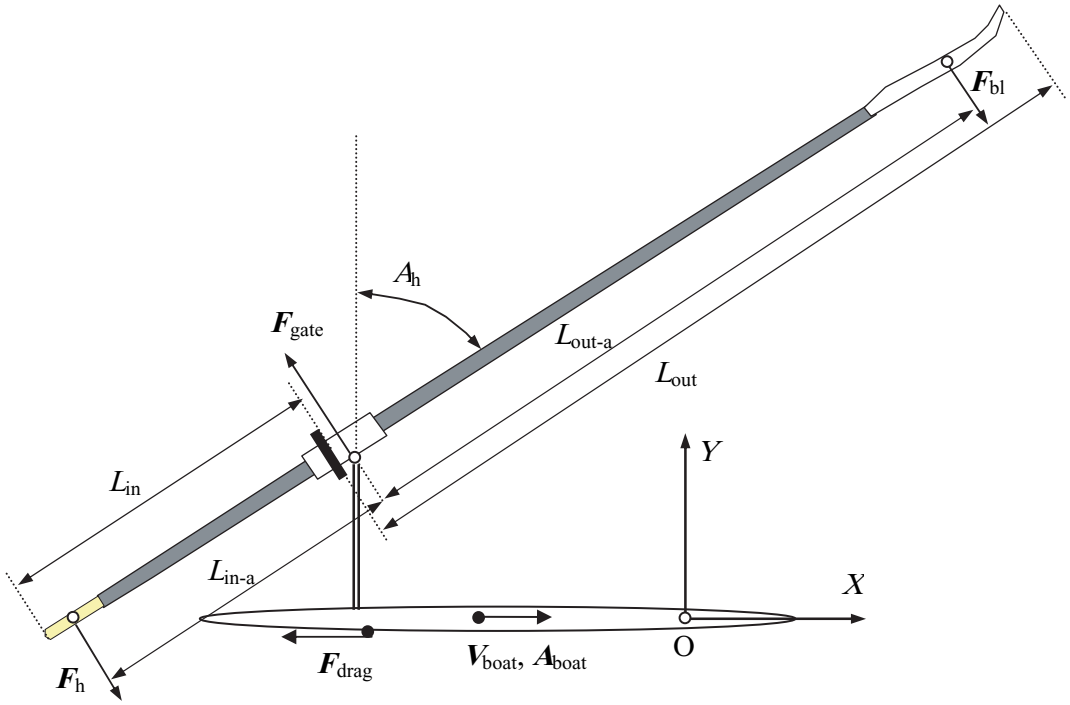

Fig. 1 Coordinate system and forces acting on the boat and oar

$$\boldsymbol{F}_{\mathrm{bl}} = \boldsymbol{F}_{\mathrm{h}} \frac{L_{\text{in-a}}}{L_{\text{out-a}}} \tag{1}$$

The effective inboard length was calculated from

$$L_{\text{in-a}} = L_{\text{in}} - \frac{L_{\mathrm{h}}}{2} + \frac{W_{\mathrm{g}}}{2} \tag{2}$$

where L_{h} is the length of handle grip (0.12 m for sculls and 0.30 m for sweep oars), L_{in} is the measured inboard length, and $W_{\mathrm{g}} = 0.04$ m is the gate width. The effective outboard length was calculated from

$$L_{\text{out-a}} = (L_{\text{oar}} - L_{\text{in}}) - \frac{L_{\text{sp}}}{2} - \frac{W_{\mathrm{g}}}{2} \tag{3}$$

where L_{oar} is the overall oar length and L_{sp} is the length of the blade spoon. It was assumed that this point is the centre of water pressure on the blade, which is a limitation of the method.

The drag force $\boldsymbol{F}_{\text{drag}}$ acting on the boat shell was derived as [**4**]

$$\boldsymbol{F}_{\text{drag}} = -\boldsymbol{K}_{\text{drag}} \boldsymbol{V}_{\text{boat}}^2 \tag{4}$$

where the drag factor $\boldsymbol{K}_{\text{drag}}$ was derived as the ratio of the integral of the blade propulsive force to the integral of the square of boat speed over the stroke cycle interval T according to

$$\boldsymbol{K}_{\text{drag}} = \frac{\int_{t=0}^{t=T} \boldsymbol{F}_{\mathrm{bl}} \cos\theta \, \mathrm{d}t}{\int_{t=0}^{t=T} \boldsymbol{V}_{\text{boat}}^2 \, \mathrm{d}t} \tag{5}$$

It was assumed that the blade force acts perpendicularly to the oar shaft, which is a limitation of the method. The propulsive force $\boldsymbol{F}_{\text{sys}}$ acting on the rower–boat system was defined as

$$\boldsymbol{F}_{\text{sys}} = \boldsymbol{F}_{\mathrm{bl}} \cos A_{\mathrm{h}} + \boldsymbol{F}_{\text{drag}} \tag{6}$$

The acceleration $\boldsymbol{A}_{\text{sys}}$ of the CM of the system was calculated as

$$\boldsymbol{A}_{\text{sys}} = \frac{\boldsymbol{F}_{\text{sys}}}{m_{\text{sys}}} = \frac{\boldsymbol{F}_{\text{sys}}}{m_{\text{boat}} + m_{\text{row}}} \tag{7}$$

where m_{sys}, m_{boat}, and m_{row} are the masses of the system, boat, and rower respectively. The acceleration $\boldsymbol{A}_{\text{row}}$ of the rower's CM was calculated as

$$\boldsymbol{A}_{\text{row}} = \frac{\boldsymbol{F}_{\text{row}}}{m_{\text{row}}} \tag{8}$$

The boat acceleration $\boldsymbol{A}_{\text{boat}}$ and propulsive force $\boldsymbol{F}_{\text{boat}}$ are related as

$$\boldsymbol{A}_{\text{boat}} = \frac{\boldsymbol{F}_{\text{boat}}}{m_{\text{boat}}} \tag{9}$$

Using the boat propulsive force $\boldsymbol{F}_{\text{boat}}$ derived in the detailed measurements and the measured boat acceleration $\boldsymbol{A}_{\text{boat}}$, it was found that the acting boat mass m_{boat} was higher than the measured boat mass. The reason for this could be the hydrodynamic added mass or other factors (aerodynamics, dynamics of oars, force on seat, etc.), which were difficult to estimate. Therefore, a correction factor was used and m_{boat} was assumed to be 30 per cent heavier than was measured.

The force $\boldsymbol{F}_{\text{row}}$ applied to the rower was derived as

$$\begin{aligned} \boldsymbol{F}_{\text{row}} &= \boldsymbol{F}_{\text{sys}} - \boldsymbol{F}_{\text{boat}} \\ &= \boldsymbol{F}_{\text{sys}} - \boldsymbol{A}_{\text{boat}} m_{\text{boat}} \end{aligned} \tag{10}$$

The deviations $\boldsymbol{V}_{\mathrm{d}}$ of the instantaneous velocities of the system, boat, and rower's CM from the average velocity of the system (and each component) during the stroke cycle were calculated as

$$\boldsymbol{V}_{\mathrm{d}} = \int \boldsymbol{A} \, \mathrm{d}t \tag{11}$$

where $\boldsymbol{A}$ is the corresponding acceleration ($\boldsymbol{A}_{\text{sys}}$, $\boldsymbol{A}_{\text{boat}}$, or $\boldsymbol{A}_{\text{row}}$). In other words, a frame of reference was used, which moved with a constant velocity equal to the average velocity of the boat during the stroke cycle. The X axis was parallel to the boat's longitudinal axis and directed towards the bow of the boat.

The velocities of the body segments were derived for use in qualitative analyses of microphases. The velocity $\boldsymbol{V}_{\text{legs}}$ of the legs was derived as the rate of variation in the measured seat position L_{s}. The velocity $\mathbf{V}_{\text{trunk/b}}$ of the trunk relative to the boat was derived in the same way using the trunk position L_{t}. The velocity $\boldsymbol{V}_{\text{trunk}}$ of the trunk relative to the seat was calculated by subtracting $\boldsymbol{V}_{\text{legs}}$ from $\boldsymbol{V}_{\text{trunk/b}}$. The velocity $\boldsymbol{V}_{\text{arms}}$ of the arms was derived as the difference between the handle velocity $\boldsymbol{V}_{\mathrm{h}}$ and $\boldsymbol{V}_{\text{trunk/b}}$, where $\boldsymbol{V}_{\mathrm{h}}$ was derived from the measured horizontal oar angle and actual inboard according to

$$\boldsymbol{V}_{\mathrm{h}} = \frac{\mathrm{d}\boldsymbol{A}_{\mathrm{h}}}{\mathrm{d}t} L_{\text{in-a}} \frac{\pi}{180} \tag{12}$$

2.5 Statistical analysis

An independent-samples t test was used to determine whether any differences between samples were significant. Significance was tested at the 0.05 level. Pearson correlation was used to define the relationships of the measured variables in the whole sample.

3 RESULTS AND DISCUSSION

3.1 Boat acceleration patterns

The magnitude of the boat acceleration $\boldsymbol{A}_{\text{boat}}$ was highly dependent on the stroke rate. Typical patterns

(Fig. 2(a)) usually had one negative peak at the catch and two positive peaks during the drive. The acceleration A_{row} of the rowers' CM (Fig. 2(b)) had two positive peaks: one just after the catch, and one in the middle of the drive. The system acceleration A_{sys} reflected the force application pattern and followed the shape of the force curve.

The negative peak of the boat acceleration A_{boat} significantly increased in magnitude with increasing stroke rate (Fig. 3(a)) (correlation with stroke rate, $r = -0.85; p < 0.01$). This can be explained by the substantial increase in inertial forces at higher stroke rates. In contrast, the first positive peak of A_{boat} increased less at higher stroke rates (Fig. 3(b)). The system acceleration A_{sys} usually increased its positive peak at higher stroke rates and decreased its negative values during recovery. This reflected the increased drag resistance at higher boat speeds.

3.2 Definition of the microphases of the stroke cycle

The accelerations of the CM of the boat, rower, and the whole system (A_{boat}, A_{row}, and A_{sys}) were used to define the microphases of the stroke cycle. These variables were chosen because they are related to the accumulation of kinetic energy in the two major components of the rower–boat system, and hence to the effectiveness of rowing technique. The word 'effectiveness' here means the capability of producing an effect, i.e. the manner of application of the rower's efforts is such that it provides the maximal average speed of the boat–rower system. The effectiveness differs from the 'efficiency', which is a ratio of the output effect (boat speed) to the input energy (rower's power) and is not discussed in this paper. While the efficiency is easy to measure, the effectiveness is difficult to quantify because the boat speed depends on many factors, which are beyond our control, namely weather conditions, rower's efforts, and capabilities. Therefore, in this article, the term effectiveness is used in a qualitative way and its evaluation is based on the overall performance of the crew.

The handle velocity V_h was used to define the overall drive phase boundaries. Figure 4 shows typical biomechanical variables of a single sculler.

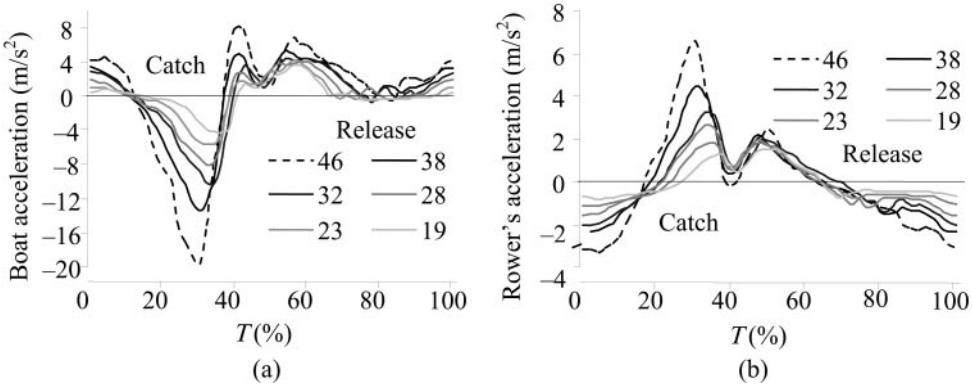

Fig. 2 Patterns of acceleration of (a) the boat and (b) the rowers' CM at different stroke rates for an Olympic Champion men's pair

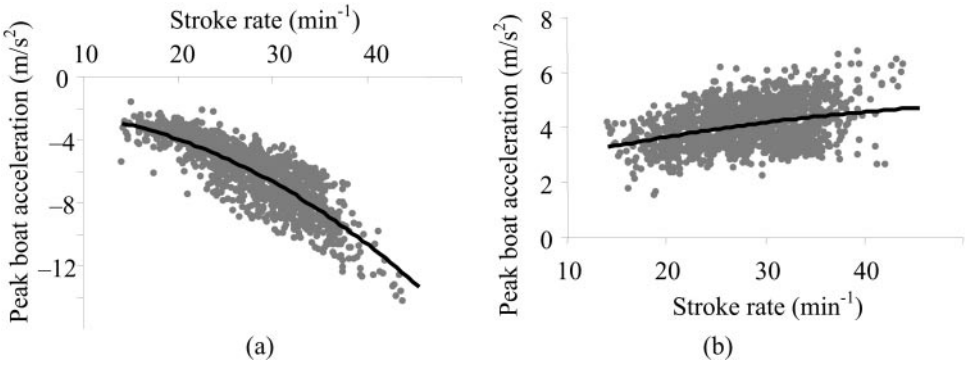

Fig. 3 Dependences of (a) the negative peak of the boat acceleration at catch and (b) the first positive peak of the boat acceleration during the drive (b) on the stroke rate

Six microphases of the drive phase (D1 to D6) and three microphases of the recovery phase (R1 to R3) were defined. Table 2 presents the microphase identifications, descriptions, and key events which define their start and end points.

3.3 Dependence of the microphase structure on the boat type, rower gender, stroke rate, and force profile

Microphases D1, D2, and D3 were slightly longer in sweep boats than in sculling boats, and microphases

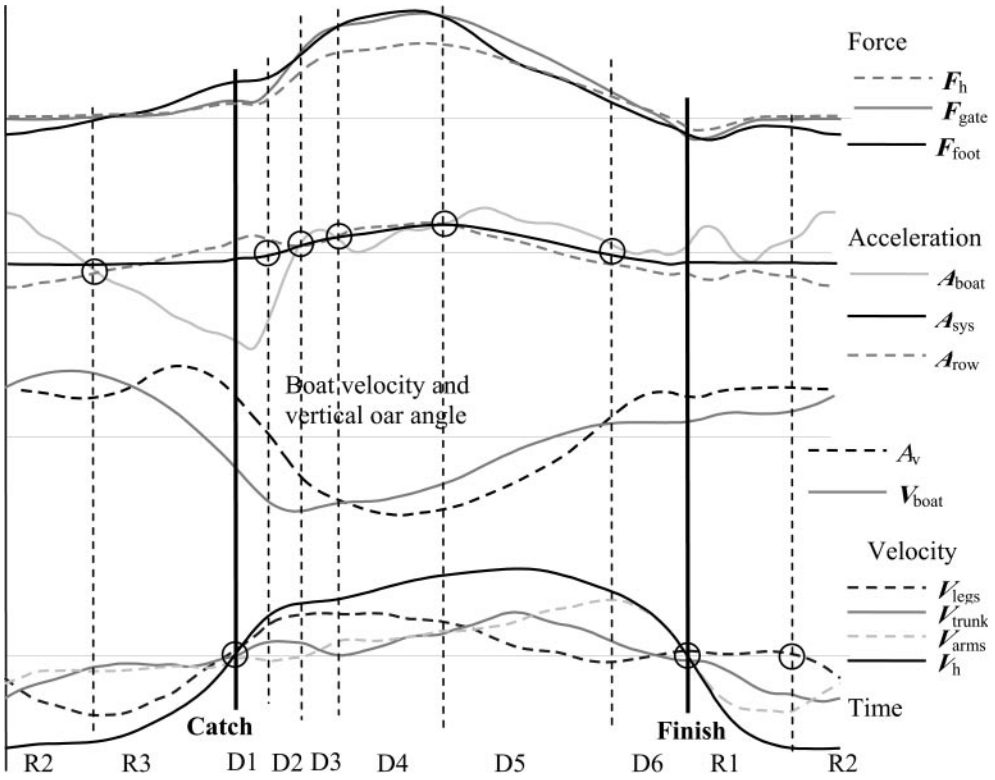

Fig. 4 Typical biomechanical parameters and microphases of the stroke cycle (M1x men's single scull; rate, 32 strokes/min). Key events are indicated as open circles

Table 2 Characteristics of the microphases of the stroke cycle

Identification	Microphase	Start event	Description
D1	Blade immersion	Catch, beginning of the drive. V_h changes sign to positive	A_{sys} and A_{boat} are negative, but A_{row} is positive. Fast increases in V_h and V_{legs}
D2	Initial rowers' acceleration	A_{sys} becomes positive. The centre of the blade crosses the water level downwards	F_h and A_{boat} increase, but A_{boat} is still negative and lower than A_{row}
D3	Initial boat acceleration	A_{boat} becomes higher than A_{row}	First positive peak of A_{boat}, which becomes higher than A_{row}. Maximum of V_{legs}
D4	Rowers' acceleration	A_{boat} decreases and becomes lower than the rower's acceleration	F_h, A_{row}, and A_{sys} increase slowly. V_{legs} decreases
D5	Boat acceleration	A_{boat} again becomes higher than A_{row}	F_h, F_{foot}, A_{row}, and A_{sys} decrease, but F_{foot} decreases faster than F_h which produces the highest A_{boat}
D6	Blade removal	A_{sys} becomes negative. The centre of the blade crosses the water level upwards	A_{row} is negative and A_{boat} is close to zero. V_h is still positive. V_{arms} is maximal
R1	Arms and trunk return	Finish, end of the drive. V_h changes sign to negative	A quick positive peak of A_{boat} and negative A_{row}, caused by transfer of the moment of inertia from the rower to the boat
R2	Legs return	Seat starts to move towards the stern. Increase in A_{boat} and decrease in A_{row}	A_{boat} is positive, but A_{row} and A_{sys} are negative. V_{legs} increases towards the stern
R3	Catch preparation	A_{boat} becomes negative and A_{row} becomes positive	F_{foot} increases, which causes a decrease in V_{legs}, deceleration of the boat, and acceleration of the rower

D4, D5, and D6 were slightly shorter ($p < 0.05$) (Fig. 5). The longer duration of D1 in sweep rowing might be due to the greater width of the sweep oar blade, which requires more time to insert into the water. The shorter duration of D2 and D3 in sculling might be due to the longer catch angles, which creates heavier effective gearing [**9**, **10**]. A heavier gearing produces a lower ratio of handle to gate forces, which creates higher acceleration of the boat compared with the rower's CM.

There were no significant differences in the durations of the D1, D2, D3, and D6 microphases among boats of different sizes (Fig. 6). D4 was significantly longer in large boats (eights and quads) and D5 was longer in small boats (singles and pairs; $p < 0.01$), but the reasons for these differences are not known.

Male crews had a longer D3 microphase than female crews did ($p < 0.01$), which is probably due to their more rapid generation of forces. Differences between other microphases for the two genders were not statistically significant.

The absolute duration of all microphases, except for D3, tended to decrease at higher stroke rates. The correlation coefficients ranged from –0.10 for D4 to –0.70 for D1. This decrease in duration was strongly correlated with a decrease in total drive time at higher stroke rates ($r = -0.87$).

The relative share of the D1 microphase within the drive phase tended to decrease at higher stroke rates ($r = -0.49$), whereas the relative share of the D6 microphase tended to increase (Fig. 7). Sculling crews tended to exhibit an absolute maximum in the relative share of the D3 microphase at a stroke rate of 30 strokes/min and sweep crews at 36 strokes/min. The reason for this phenomenon is not known.

To analyse the relationship between microphase proportions and the force curve profile, there was the time from the catch until the moment when the force $\boldsymbol{V}_h$ achieved 10 per cent, 20 per cent, ..., 100 per cent of its maximal value. The following statistically significant relationships were found (Fig. 8).

1. The D1 period had the strongest positive correlation with the time for achieving 30 per cent of the maximal force ($r = 0.91$; $p < 0.001$).
2. D3 had the strongest negative correlation with the time for achieving 70 per cent ($r = -0.45$; $p < 0.05$) and 80 per cent ($r = -0.46$; $p < 0.05$) of the maximal force.
3. D6 had a negative correlation with the time taken to achieve 30 per cent of the maximal force ($r = -0.46$; $p < 0.05$).

3.4 Case study: the importance of the D3 microphase

To discuss the influence of different rowing technique factors on the temporal structure of the drive

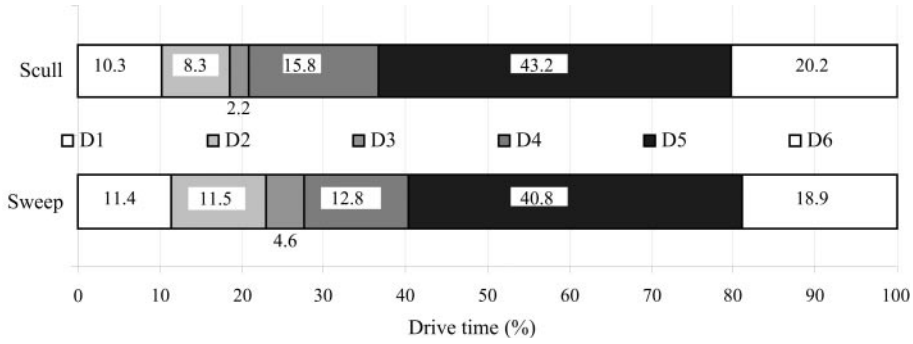

Fig. 5 Time structures of the drive phase in sweep and sculling crews

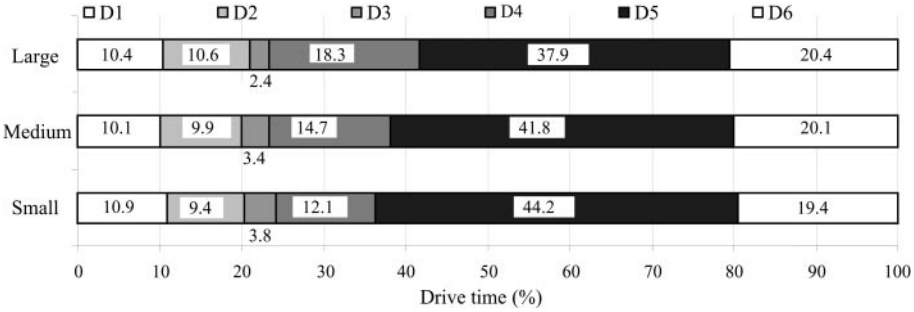

Fig. 6 Time structures of the drive phase in small (1× single scull, 2− pair), medium (2× double scull, 4− four) and large (4× quadruple scull, 8+ eight) boat types

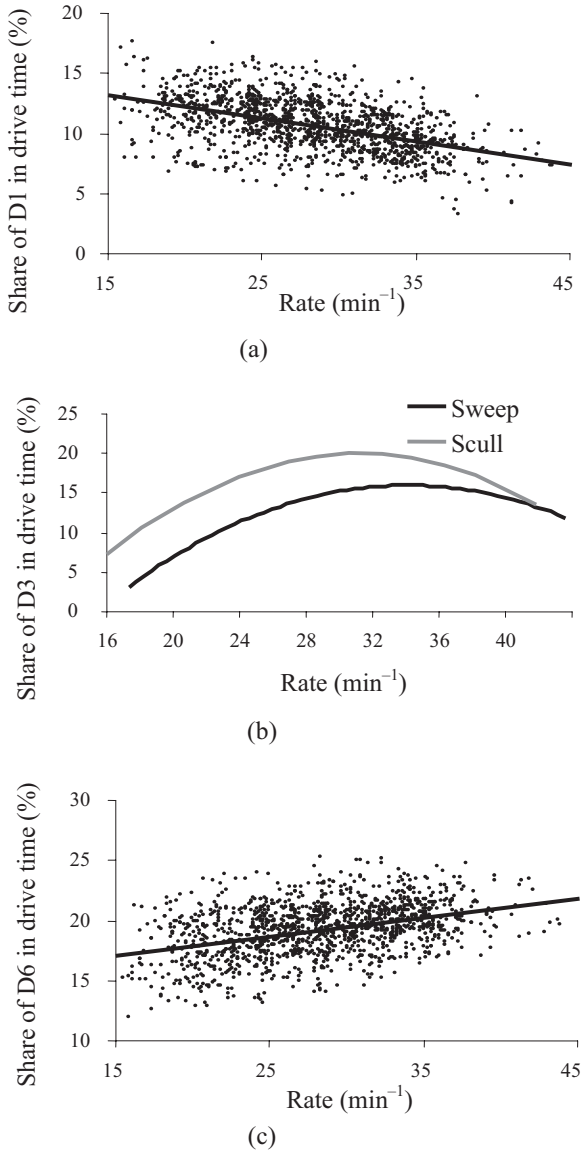

Fig. 7 Dependences of the microphase time shares in the drive time on the stroke rate: (a), (b) linear trends; (c) second-order polynomial trend

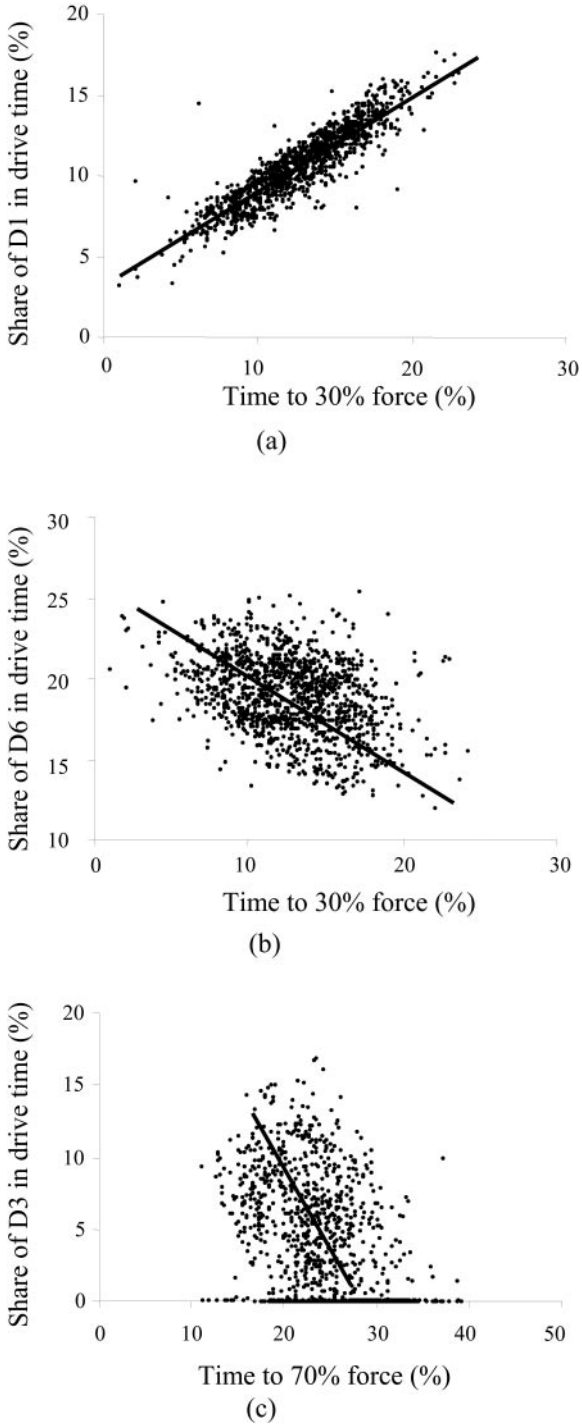

Fig. 8 Dependences of the proportion of microphase within the drive phase on the stroke rate with linear trend lines

phase, two crews of international level were selected. The first crew consisted of Olympic Champions and was considered by experts to be highly technically effective. The second crew was in the finals of the World Championship, had very good physiological work capacity, but could not achieve excellent performance on the water. Both samples were taken at a stroke rate close to 32 strokes/min. The first crew produced a much quicker rise in the handle force (Fig. 9(a)), achieving 70 per cent of their maximal force at 23.1 per cent of the drive time. The second crew had a relatively flatter force curve (70 per cent of the maximal force at 29.1 per cent of the drive time), but higher maximal and average forces.

The faster rise in the force of the first crew coincides with a faster increase in the velocity $\boldsymbol{V}_{\text{legs}}$ of the legs (Fig. 9(d)) (the maximal velocity of the legs occurred at 22.4 per cent of the drive time) and was accompanied by a steady increase in the trunk velocity $\boldsymbol{V}_{\text{trunk}}$ (Fig. 9(f)). The second crew had a slower velocity of the legs in the first half of the drive

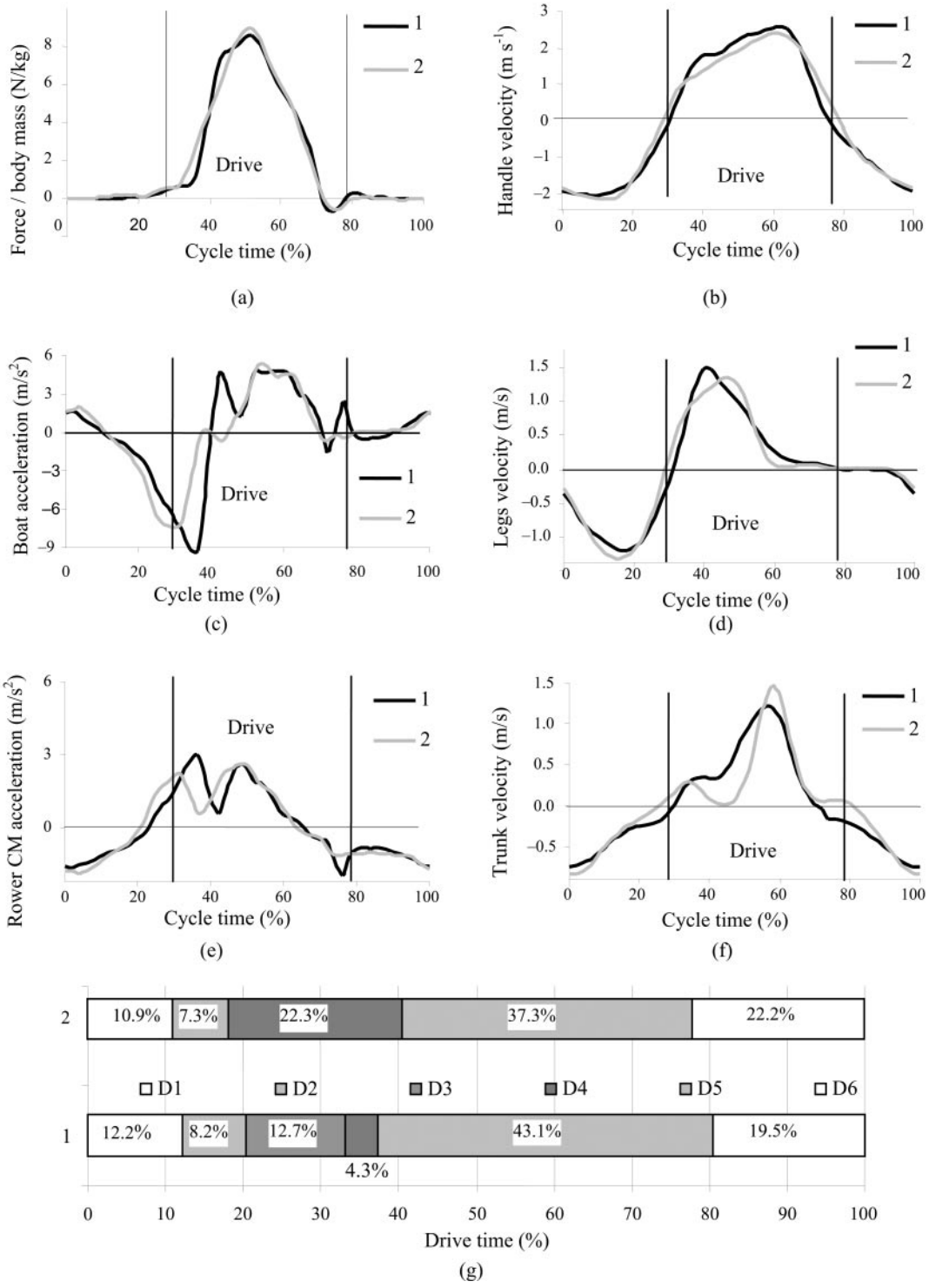

Fig. 9 Biomechanical parameters and temporal structures of the drive phase for two examples of rowing technique

(the maximal velocity of the legs at 32.2 per cent of the drive time) and a double-peaked trunk speed profile. Consequently, the handle velocity $\boldsymbol{V}_{\mathrm{h}}$ of the first crew increased more rapidly during the first half of the drive (Fig. 9(b)).

The boat acceleration $\boldsymbol{A}_{\mathrm{boat}}$ of the first crew had a deeper and later negative peak at the catch (8.4 m/s^2 compared with 7.3 m/s^2 in the second crew), but a much quicker increase afterwards (Fig. 9(c)). The first peak of $\boldsymbol{A}_{\mathrm{boat}}$ was 2.7 m/s^2 in the first crew, but only 0.3 m/s^2 in the second crew, which had $\boldsymbol{A}_{\mathrm{boat}}$ drop below zero after the first peak.

The first crew had a higher acceleration $\boldsymbol{A}_{\mathrm{row}}$ of the rower's CM at the catch, but the second crew

accelerated their body mass more intensively during the middle of the drive (Fig. 9(e)). As a result, the second crew did not have microphase D3 (initial boat acceleration) at all, but it had a much longer D4 (main rowers' acceleration).

4 DISCUSSION AND IMPLICATIONS: TEMPORAL ANALYSIS AND THE EFFECTIVENESS OF THE ROWING TECHNIQUE

The main measure of rowing performance is the average speed of the rower–boat system. Rowers cannot increase the system velocity during the recovery phase, because its deceleration is affected by such environmental factors as water and air resistance. The drive phase is the only time when rowers can increase the system velocity (more precisely, only that part of the drive when the propulsive force is higher than the drag force). The higher acceleration of the system during the drive phase means a higher average speed and hence better performance. The system accumulates kinetic energy during the drive phase and loses it during the recovery phase.

The gain dE in kinetic energy of any body can be defined using the equation

$$\mathrm{d}E = \frac{m\boldsymbol{v}_2^2}{2} - \frac{m\boldsymbol{v}_1^2}{2} = \frac{m}{2}(\boldsymbol{v}_2^2 - \boldsymbol{v}_1^2) \tag{13}$$

where m is the mass of the body and $\boldsymbol{v}_1$ and $\boldsymbol{v}_2$ are the start and end velocities respectively of the body's CM.

The mass of the rower is significantly greater than that of the boat (the ratio ranges from 400 per cent in lightweight women to 600 per cent in heavyweight men). To maximize the average speed, the rowers must maximize the gain in kinetic energy, which can be achieved most effectively by means of acceleration of the heaviest part of the system (i.e. the rower's CM). Therefore the effectiveness of the rowing technique is related to the magnitude and timing of the acceleration of the rower's CM.

The acceleration of any body depends on the force acting on it. The force $\boldsymbol{F}_{\mathrm{row}}$ applied to the rower's CM (Fig. 10) is equal to the sum of the foot-stretcher reaction force $\boldsymbol{F}_{\mathrm{r.foot}}$, which is positive, i.e. pushes the athlete's CM forwards, and the handle reaction force $\boldsymbol{F}_{\mathrm{r.handle}}$, which is negative, i.e. pulls the rower backwards, according to

$$\boldsymbol{F}_{\mathrm{row}} = \boldsymbol{F}_{\mathrm{r.foot}} + \boldsymbol{F}_{\mathrm{r.handle}} \tag{14}$$

Both these reaction forces have the same magnitude and the opposite direction to the action forces $\boldsymbol{F}_{\mathrm{foot}}$ and $\boldsymbol{F}_{\mathrm{h}}$.

The force $\boldsymbol{F}_{\mathrm{boat}}$ applied to the boat hull is equal to the sum of the gate force $\boldsymbol{F}_{\mathrm{gate}}$, the stretcher force $\boldsymbol{F}_{\mathrm{foot}}$, and the drag force $\boldsymbol{F}_{\mathrm{drag}}$ (ignoring the small seat frictional force) according to

$$\boldsymbol{F}_{\mathrm{boat}} = \boldsymbol{F}_{\mathrm{gate}} + \boldsymbol{F}_{\mathrm{foot}} + \boldsymbol{F}_{\mathrm{drag}} \tag{15}$$

Therefore, emphasis on the boat acceleration requires rowers to produce a higher gate force $\boldsymbol{F}_{\mathrm{gate}}$ (and a correspondingly higher handle force $\boldsymbol{F}_{\mathrm{h}}$) and to push on the stretcher less. Vice versa, emphasis on accelerating the rower's CM requires a higher stretcher force $\boldsymbol{F}_{\mathrm{foot}}$ and lower handle force $\boldsymbol{F}_{\mathrm{h}}$. Graphs of the gate and stretcher forces in Fig. 4 confirm that this switching of the emphasis happens twice during the drive.

The stretcher force $\boldsymbol{F}_{\mathrm{foot}}$ is the primary focus during the drive because it increases the acceleration $\boldsymbol{A}_{\mathrm{row}}$ of the rower's CM, which provides the most significant accumulation of kinetic energy and hence increases the system's average speed.

However, the effectiveness of the rower's push on the stretcher is affected by the boat velocity at that time. If the stretcher (boat) has a higher velocity, then the rowers can accelerate their CM more efficiently than if the boat is moving more slowly. It can be speculated that using the elastic energy stored in the

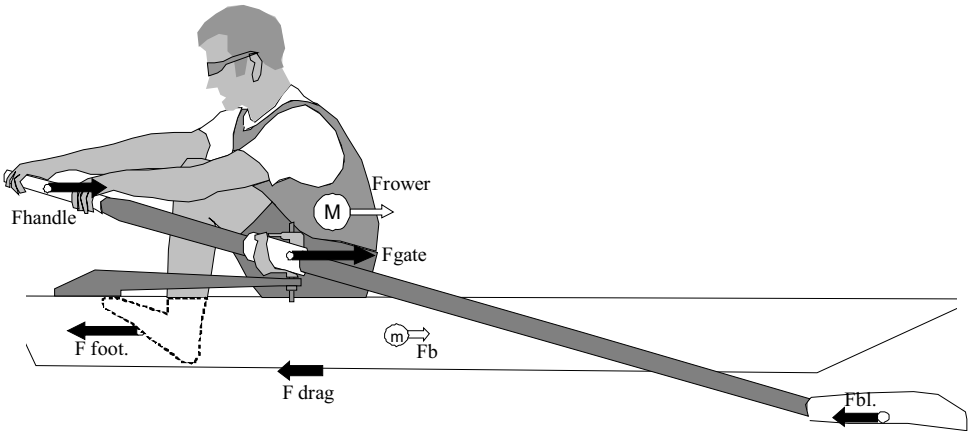

Fig. 10 The main forces in the rower–boat–oar system

oar handle and in the rower's tendons and muscles can play a significant role at the beginning of the drive. However, this topic is beyond the scope of this paper and can be the subject of further research. The use of elastic energy is similar to jumping on a trampoline; the point of support moves in the direction of acceleration of the athlete's CM and adds the velocity of the support point to that of the athlete's CM, which makes the acceleration more effective. The presence of D3 could be called a 'trampolining effect' and can be regarded as an important indicator of the effectiveness of the rowing technique [**11**]. In addition, earlier force application could help to utilize the hydrolift effect better [**12**].

The practical implications of the microphases of the drive phase are as follows.

During microphases D1 and D2 the rowers emphasize push with legs because they have to change the direction of their movement from the stern to the bow at the catch. This accelerates their body mass and decelerates the boat. At the same time, the blade obtains a grip on the water.

During D3 the rowers emphasize pulling the handle to accelerate the boat. This creates a faster-moving support on the stretcher. This microphase is important for performing an effective drive phase. It was found that in 43 per cent of the crews this microphase was absent, but a longer duration of D3 does not mean better technique because D3 was the longest in some low-level crews (according to an expert's opinion).

During D4 the rowers emphasize the stretcher push again to accelerate themselves and hence to accumulate kinetic energy. The effectiveness of this microphase depends on the amount of boat velocity gained during the previous microphase D3, and on a fast powerful leg drive.

The microphases D5 and D6 occur after the legs are substantially extended and use trunk and arm work instead. The force levels and the total system acceleration decrease, but the stretcher force decreases more quickly and becomes negative (pull on the stretcher). This puts emphasis on the boat acceleration again. The rower's CM acceleration becomes negative, which means transferring kinetic energy from the rower's mass to the boat.

5 CONCLUSIONS

The phenomenon of a double peak in the boat acceleration during the drive phase can be explained by double switching of the emphasis from pushing the stretcher (more rowers' CM acceleration) to pulling the handle (more boat hull acceleration). Acceleration of the boat and of the rowers' CM, and the velocity of the oar handle, were used to define the temporal structure of the stroke cycle. Six microphases were defined during the drive phase and three microphases were defined during the recovery phase. The presence of the microphase D3 (initial boat acceleration) was an important indicator of the effectiveness of a rower's technique. The initial boat acceleration creates a faster-moving platform for the stretcher to allow better acceleration of the rower's CM.

ACKNOWLEDGEMENT

This research project was kindly supported by the Australian Institute of Sport and Rowing Australia.

REFERENCES

1 **Bartlett, R.** *Sport biomechanics: preventing injury and improving performance*, 1999, pp. 11–21 (Routledge, New York).
2 **Toussaint, H. M.** and **Beek, P. J.** Biomechanics of competitive front crawl swimming. *Sports Med.*, 1992, **13**, 8–24.
3 **James, S. L.** and **Brubaker, C. E.** Biomechanical and neuromuscular aspects of running. *Exercise Sport Sci. Rev.*, 1973, **1**, 189–216.
4 **Dal-Monte, A.** and **Komor, A.** Rowing and sculling mechanics. In *Biomechanics of sport* (Ed. C. L. Vaughan), 1989, pp. 53–119 (CRC Press, Boca Raton, Florida).
5 **Rodriguez, R. J., Rogriguez, R. P., Cook, S. D.,** and **Sandborn, P. M.** Electromyographic analysis of rowing stroke biomechanics. *J. Sports Med. Phys. Fitness*, 1990, **30**, 103–108.
6 **Shimoda, M., Kawakami, Y.,** and **Fukunaga, T.** An application of acceleration analysis to evaluation of a rowing technique. In Proceedings of the 13th International Symposium on *Biomechanics in sports* (Ed. T. Bauer), Thunder Bay, Ontario, Canada, 18–22 July 1995, pp. 95–100 (Lakehead University, Thunder Bay, Ontario).
7 Fédération Internationale des Sociétés d'Aviron (International Rowing Federation), FISA rules of racing and related bye-laws, Part IV, Boats and construction, 2005–2006, pp. 60–66, available from http://www.worldrowing.com/medias/docs/media_352459.pdf.
8 Geoscience Australia, Applying geoscience to Australia's most important challenges, 2009, available from http://www.geo.gov.au.
9 **Kleshnev, V.** Technology for technique improvement. In *Rowing faster* (Ed. V. Nolte), 2004, pp. 209–228 (Human Kinetics, Champaign, Illinois).
10 **Kleshnev, V.** Facts. Did you know that . . . . *Rowing Biomech. Newslett.*, 2007, **7**(72), available from http://www.biorow.com/RBN_en_2007_files/2007RowBiomNews03.pdf.

11 Kleshnev, V. Ideas. *Rowing Biomech. Newslett.*, 2006, **6**(2), available from http://www.biorow.com/RBN_en_2006_files/RowBiomNews03.pdf.
12 Pulman, C. The physics of rowing, 2008, available from http://www.atm.ox.ac.uk/rowing/physics/rowing.pdf.

APPENDIX

Notation

A_h	horizontal oar angle
A_v	vertical oar angle
$\boldsymbol{A}_{boat}$	boat acceleration
$\boldsymbol{A}_{row}$	acceleration of the centre of mass of the rower
$\boldsymbol{A}_{sys}$	acceleration of the centre of mass of the rower–boat system
CM	centre of mass
dE	gain in kinetic energy of any body
$\boldsymbol{F}_{bl}$	blade force
$\boldsymbol{F}_{boat}$	force acting on the boat
$\boldsymbol{F}_{drag}$	drag force
$\boldsymbol{F}_{foot}$	foot-stretcher force
$\boldsymbol{F}_{gate}$	gate force
$\boldsymbol{F}_h$	normal component of the force applied to the handle of the oar
$\boldsymbol{F}_{r.foot}$	foot-stretcher reaction force
$\boldsymbol{F}_{r.handle}$	handle reaction force
$\boldsymbol{F}_{row}$	force acting on the centre of mass of the rower
$\boldsymbol{F}_{sys}$	force acting on the centre of mass of the rower–boat system
$\boldsymbol{K}_{drag}$	drag factor
L_h	length of the hand grip
L_{in}	measured inboard length
$L_{in\text{-}a}$	actual inboard length
L_{oar}	overall oar length
$L_{out\text{-}a}$	actual outboard length
L_s	seat position
L_{sp}	length of the blade spoon
L_t	position of the top of the trunk
m	mass of the body
m_{boat}	mass of the boat
m_{row}	mass of the rower
m_{sys}	mass of the rower–boat system
$\boldsymbol{v}_1$	start velocity
$\boldsymbol{v}_2$	end velocity
$\boldsymbol{V}_{arms}$	velocity of the arms
$\boldsymbol{V}_{boat}$	velocity of the boat
$\boldsymbol{V}_d$	deviation of the instantaneous velocity from the average velocity
$\boldsymbol{V}_{legs}$	velocity of the legs
$\boldsymbol{V}_{trunk}$	velocity of the trunk
$\boldsymbol{V}_{trunk/b}$	velocity of the trunk relative to the boat
W_g	width of the gate